

CLIMATE RISK COUNTRY PROFILE

COMOROS



THE WORLD BANK
IBRD • IDA | WORLD BANK GROUP

COPYRIGHT

© 2025 by the World Bank Group
1818 H Street NW, Washington, DC 20433
Telephone: 202-473-1000; Internet: www.worldbank.org

This work is a product of the staff of the World Bank Group (WBG) and with external contributions. The opinions, findings, interpretations, and conclusions expressed in this work are those of the authors and do not necessarily reflect the views or the official policy or position of the WBG, its Board of Executive Directors, or the governments it represents.

The WBG does not guarantee the accuracy of the data included in this work and does not make any warranty, express or implied, nor assume any liability or responsibility for any consequence of their use. This publication follows the WBG's practice in references to member designations, borders, and maps. The boundaries, colors, denominations, and other information shown on any map in this work, or the use of the term "country" do not imply any judgment on the part of the WBG, its Boards, or the governments it represents, concerning the legal status of any territory or geographic area or the endorsement or acceptance of such boundaries.

The mention of any specific companies or products of manufacturers does not imply that they are endorsed or recommended by the WBG in preference to others of a similar nature that are not mentioned.

RIGHTS AND PERMISSIONS

The material in this work is subject to copyright. Because the WBG encourages dissemination of its knowledge, this work may be reproduced, in whole or in part, for noncommercial purposes as long as full attribution to this work is given.

Please cite the work as follows: Climate Risk Profile: Comoros (2025): The World Bank Group.

Any queries on rights and licenses, including subsidiary rights, should be addressed to World Bank Publications, The World Bank Group, 1818 H Street NW, Washington, DC 20433, USA; fax: 202-522-2625; e-mail: pubrights@worldbank.org.

Cover Photos: © Dimitri Dim / Pexels.com, "Aerial View of Canoes on Shore." January 30th, 2019. Free to use under the [Pexels License](#). © Amau Iramu / Unsplash.com, "An aerial view of a city with lots of house." June 4, 2024. Free to use under the [Unsplash License](#).

Graphic Design: [Circle Graphics, Inc.](#), Reisterstown, MD.

ACKNOWLEDGEMENTS

This profile is part of a series of Climate Risk Country Profiles developed by Climate Change Group of the World Bank Group (WBG). The country profiles aim to present a high-level assessment of the climate risks faced by countries, including rapid-onset events and slow-onset changes in climate conditions, many of which are already underway, as well as summarize relevant information on policy and planning efforts at the country level.

The country profile series are designed to be a reference source for development practitioners to better integrate detailed climate data, physical climate risks and need for resilience in development planning and policy making.

This effort is managed and led by MacKenzie Dove (Technical Lead, CCKP, WBG) and Pascal Saura (Task Team Lead, CCKP, WBG).

This profile was written by Anna Cabré Albós (Climate Change Consultant, CCKP, WBG).

Unless otherwise noted, data is sourced from the WBG's [Climate Change Knowledge Portal \(CCKP\)](#), the WBG's designated platform for climate data. Climate, climate change and climate-related data and information on CCKP represents the latest available data and analysis based on the latest [Intergovernmental Panel on Climate Change \(IPCC\)](#) reports and datasets. The team is grateful for all comments and suggestions received from climate and development specialists, as well as climate research scientists and institutions for their advice and guidance on the use of climate related datasets.

CONTENTS

FOREWORD	1
KEY MESSAGES	2
COUNTRY OVERVIEW	3
CLIMATE OVERVIEW	6
TEMPERATURE AND PRECIPITATION HISTORICAL AND PROJECTED TRENDS	7
Historical Temperature Changes	8
Projected Temperature Changes	8
Historical Precipitation Changes	9
Projected Precipitation Changes	10
IMPACTS OF A CHANGING CLIMATE	12
Hot Days	12
Hot Nights	12
Humid Heat	13
Drought	14
Extreme Precipitation	15
Sea Surface Temperatures	17
Sea Level Rise	17
Tropical Cyclones	18
Blue Economy Impacts	22

FOREWORD

Development progress has stalled in many countries amid low growth, increased fragility and conflict, pandemic-related setbacks, and the impacts of climate change. Droughts, extreme heat, flooding and storms push millions into poverty annually, causing unemployment and risking unplanned internal and cross-border migration. Every year, an estimated 26 million people fall behind due to extreme weather events and natural disasters. These shocks have the potential to push a total of 130 million into poverty by 2030.

The World Bank Group (WBG) is supporting countries to meet these challenges. As part of our vision to end poverty on a livable planet, we are investing in development projects that improve quality of life while creating local jobs, strengthening education, and promoting economic stability. We are also helping people and communities adapt and prepare for the unpredictable and life-changing weather patterns they are experiencing, ensuring that limited development resources are used wisely and that the investments made today will be sustainable over time.

Having access to data that is accurate and easily understandable is of course critical to making informed decisions. This is where the report you are about to read comes in.

Climate Risk Country Profiles offer country-level overviews of physical climate risks across multiple spatiotemporal scales. Each profile feeds into the economy-wide [Country Climate and Development Reports](#) and draws its insights from the [Climate Change Knowledge Portal](#), the WBG's 'one-stop-shop' for foundational climate data.

Guided by World Bank Group data and analytics, developing countries can conduct initial assessments of climate risks and opportunities that will inform upstream diagnostics, policy dialogue, and strategic planning. It is my sincere hope that this country profile will be used to inform adaptation and resilience efforts that create opportunities for people and communities around the world.



Valerie Hickey, PhD

Global Director
Climate Change Group
World Bank Group

KEY MESSAGES

The main climate change risks for Comoros are sea level rise, storm surge, coastal flooding, increased temperatures and extreme weather events, and the potential decline of marine ecosystems.

Historical trends in temperature: Over the past few decades, mean air surface temperatures have risen significantly, with a notably faster increase observed in the last three decades (0.22°C /decade) compared to earlier periods. This translates into more days with extreme maximum temperatures, more summer days, and more days with dangerous combined heat and humidity.

Projected trends in temperature: Comoros's temperatures are projected to increase further into the future for all the scenarios. Under SSP3-7.0, the mean temperature nationwide increases from 25.31°C during the historical reference period of 1995–2014 to 26.39°C (26.10°C, 26.98°C) for the period 2040–2059. Comoros historically experienced few hot days ($T_{\max} > 30^{\circ}\text{C}$), but projections indicate that by 2040–2059, it will experience 23 hot days annually, rising to 100 days per year by 2080–2099. Historically, the island experienced approximately 38 tropical nights per year ($T_{\min} > 26^{\circ}\text{C}$). Under the SSP3-7.0 scenario, projections show an increase to 120 nights (4 months) by mid-century (2040–2059), and 223 nights (over 7 months) by the end of the century (2080–2099). The heat index, measuring heat and humidity, is also expected to rise by the end of the 21st century, reaching up to three months per year by 2081–2100 of heat index $> 35^{\circ}\text{C}$.

Historical trends in precipitation: Precipitation patterns have become more erratic, with greater variability year-to-year compared to the multi-year variability seen before 1975. While the long-term trend points toward drying, the past three decades have shown a slight, though not significant, increase in rainfall.

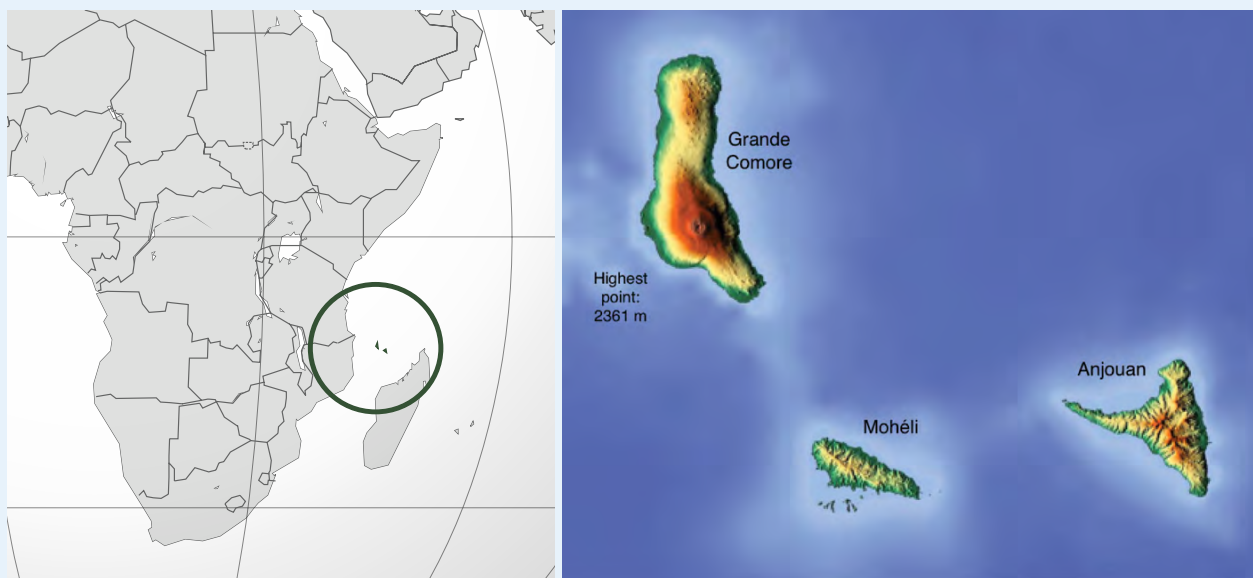
Projected trends in precipitation: In Comoros, climate change is not projected to significantly affect average annual precipitation levels, and both interannual variability and inter-model dispersion remain notably high. Seasonally, projections suggest a future climate characterized by a slightly wetter wet season, a drier dry season, and a delayed onset of the rainy season. Extreme precipitation events with return periods of 100 years are projected to occur 74% more frequently by mid-century (2035–2064) under the SSP3-7.0 scenario, compared to historical data from 1985–2014.

Comoros and its tropical marine ecosystems will face the impacts of rising temperatures and sea levels. Coupled with cyclones and more extreme precipitation events, this will lead to increased sea level surges and a higher risk of coastal inundation.

COUNTRY OVERVIEW

The Comoros is an archipelagic nation in Southeastern Africa, located at the northern end of the Mozambique Channel in the Indian Ocean, about 290 km off the eastern coast of Africa, northwest of Madagascar, near 12°S and 44°E. The country consists of three main islands, listed from northwest to southeast: Grande Comore (N'gazidja), Mohéli (Mwali), and Anjouan (Ndzuwani) (**Fig. 1**).

FIGURE 1. Map Indicating the Location of the Comoros Archipelago¹ and Topography². The Archipelago's Topography Plays a Crucial Role in Shaping Wind Patterns, Climate, and the Impacts of Sea Level Rise.



The Comorian archipelago is often referred to as the “perfumed islands” due to its fragrant plant life. These volcanic islands emerged from the depths of the Indian Ocean, and their coastlines are often framed by coral reefs that provide a barrier against the ocean's waves. The beaches are broad and sandy, punctuated by clusters of coconut palms or mangrove trees, while some areas are marked by rough lava flows or smooth, eroded volcanic rocks, remnants of ancient eruptions³.

Grande Comore, the largest and highest of the islands, is dominated by Mount Karthala, an active volcano standing at 2,361 meters, the highest point in the country. Mount Karthala has erupted more than a dozen times in the last 200 years. The capital city, Moroni, lies along the west coast in the volcano's shadow, while the northern town of Mitsamiouli sits by the coast. The island's terrain is largely rocky, with shallow soils and a plateau rising to 600 meters north of the volcano.

¹ Wikipedia [https://en.wikipedia.org/wiki/List_of_companies_of_the_Comoros#/media/File:Comoros_\(orthographic_projection\).svg](https://en.wikipedia.org/wiki/List_of_companies_of_the_Comoros#/media/File:Comoros_(orthographic_projection).svg)

² Wikipedia https://en.m.wikipedia.org/wiki/File:Comoros_location_map_Topographic.png

³ Britannica <https://www.britannica.com/place/Comoros>

Mohéli, the smallest of the islands, is characterized by a plateau averaging 300 meters in elevation, with a ridge on the western end rising above 790 meters. The island's fertile valleys and forested hillsides support lush vegetation. Its key towns are Fomboni in the north and Nioumachoua to the southwest.

Anjouan, a triangular island, is dominated by the volcanic massif of Mount Ntingui, which reaches 1,580 meters. Although the soil is generally fertile, significant erosion has occurred over time, rendering large portions of the island unfit for agriculture.

The Comoros has a high population density, with around 465 inhabitants per square kilometer, and a young population, as over half (53%) of its 869,595 people (as of 2020) are under the age of 20⁴. More than two-thirds of the population live in rural areas, with the majority concentrated on the two larger islands. Grande Comore is home to about half of the population, Anjouan houses roughly two-fifths, and Mohéli has less than one-tenth. The capital city, Moroni, is the largest urban center in the country (**Fig. 2**).

Poverty is widespread in the Comoros, with 40% of the population living below the poverty line⁵. Classified by the UN as one of the least developed countries (LDC), Comoros has an economy largely based on subsistence agriculture and fishing. Subsistence farming produces crops such as cassava, sweet potatoes, bananas, and mountain rice (dry-field), though much of the country's food supply must be imported. Livestock includes chickens, goats, cattle, and sheep. Plantations across the islands are dedicated to crops like vanilla (mainly on Grande Comore and Anjouan), perfume plants such as ylang-ylang (especially on Anjouan), coconuts (primarily on Mohéli), as well as coffee, cloves, cacao, and other cash crops.

Fishing remains a small-scale industry, with abundant tuna in Comorian waters mostly exploited by foreign nations. Tourism has not reached its full potential.

As a small island state, Comoros's main climate risks are sea level rise, storm surge, flooding, increased temperatures and extreme precipitation weather events, which have consequences on health, agriculture, water management, and marine ecosystems. In addition to the impacts of climate change, Mauritius faces deforestation, due to the expansion of agriculture.

Comoros presented its second National Communication in 2012⁶, and the updated Nationally Determined Contribution⁷ in 2021, which outlines key climate adaptation strategies focused on protecting agriculture, biodiversity and ecosystems, forestry, coastal zones, and prioritizing water, health and infrastructure.

⁴ World Bank Data

⁵ World Bank Data

⁶ Second National Communication <https://unfccc.int/documents/75460>

⁷ Updated National Determined Contribution, 2021 (French) https://unfccc.int/sites/default/files/NDC/2022-06/CDN_r%C3%A9vis%C3%A9e_Comores_vf.pdf

FIGURE 2. Population Density (per 10,000 square meters) in Comoros, 2020⁸



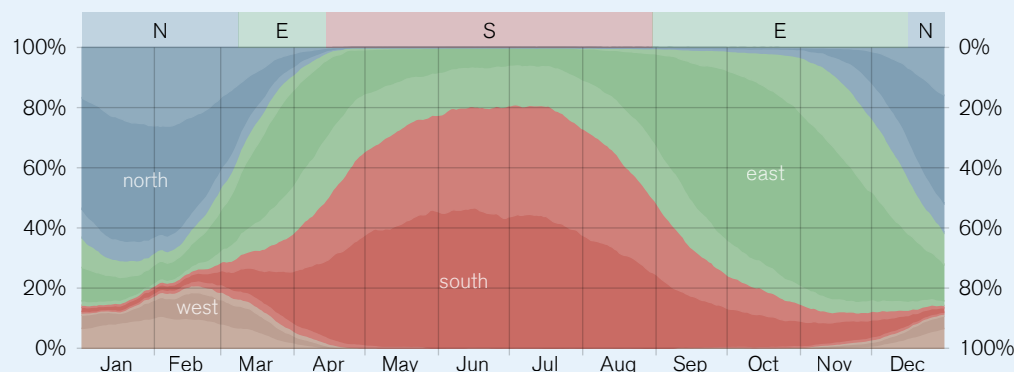
⁸ Comoros: Main Health Facilities and Population Density Map (May 2020) <https://www.unocha.org/publications/map/comoros/comoros-main-health-facilities-and-population-density-map-may-2020>

CLIMATE OVERVIEW

Data overview: Historically, observed data is derived from the Climatic Research Unit, University of East Anglia (CRU), CRU TS version 4.08 gridded dataset (data available 1901–2023). The CRU dataset relies on stations data.

Comoros has a tropical climate with a hot, rainy season from December to April, characterized by northeast winds that bring frequent storms and cyclones. The dry season lasts from May to November, marked by southeast winds, lower rainfall, and cooler temperatures (**Figs. 3 and 4**).

FIGURE 3. Average Historical Wind Direction in Comoros⁹: “The Percentage of Hours in Which the Mean Wind Direction is from Each of the Four Cardinal Wind Directions, Excluding Hours in Which the Mean Wind Speed is Less Than 1.0 mph. The Lightly Tinted Areas at the Boundaries are the Percentage of Hours Spent in the Implied Intermediate Directions (northeast, southeast, southwest, and northwest).”



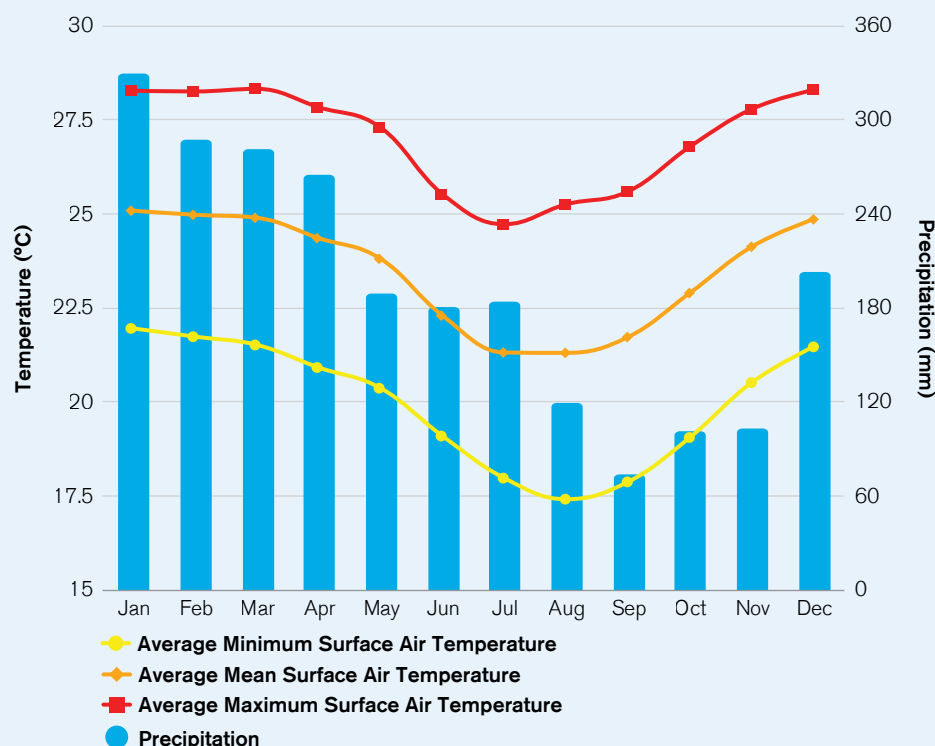
Rainfall peaks in January at 313 mm and reaches its lowest point in September at 64 mm. Precipitation is highest on the windward northeast sides of the islands during the rainy season, with annual rainfall across the archipelago averaging 2,098 mm. However, there is considerable variation in rainfall across the islands, ranging from 1,000 to 5,000 mm, influenced by altitude and wind patterns. The islands are known for their microclimates, with rainfall decreasing from west to east. Grande Comoro receives about 2,315 mm annually, Mohéli gets 2,005 mm, and Anjouan receives 1,631 mm.

The average temperature across the archipelago is 23.7°C, with Mohéli being about 1°C warmer on average. July is the coolest month, with an average temperature of 21.6°C, ranging from 18.3°C to 25.0°C. January, the warmest and wettest month, sees temperatures between 22.2°C and 28.4°C, with an average of 25.3°C.

Comoros is affected by several key modes of natural climate variability in the Indian Ocean, which shape its weather patterns, rainfall, temperatures, and cyclone activity. The global El Niño-Southern Oscillation (ENSO) most often leads to warmer-than-usual conditions and rainier conditions, while la Niña impact is less pronounced and variable. Other modes of variability are the Indian Ocean Dipole (IOD) or the Indian Ocean Basin Mode (IOBM). Short-term

⁹ Weather Spark <https://weatherspark.com/y/150243/Average-Weather-in-Comoros-Year-Round?>

FIGURE 4. Monthly Historical Climatology of Average Temperature (minimum, average, and maximum) and Total Precipitation (1991–2020) for Comoros (CRU dataset)



variability is influenced by monsoon and cyclone systems and the Inter-Tropical Convergence Zone (ITCZ). The ITCZ moves north and south with the seasons, and when it is positioned closer to Comoros (typically in the austral summer, between November and April), it brings heavy rainfall.

TEMPERATURE AND PRECIPITATION HISTORICAL AND PROJECTED TRENDS

Data overview: Historical observed data is derived from the ERA5 reanalysis collection from ECMWF (1950–2023). Modeled future climate data is derived from CMIP6, the Coupled Model Intercomparison Project, Phase 6. This risk profile focuses primarily on SSP3-7.0¹⁰, which projects a doubling of

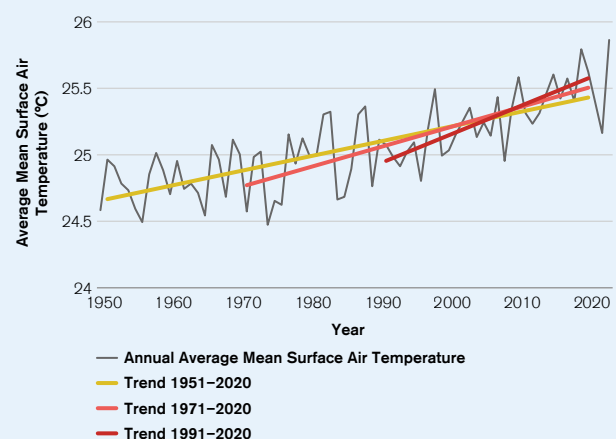
¹⁰ Climate scientists may prioritize SSP4.5 and SSP8.5 to cover a range of potential futures, but SSP8.5 is frequently avoided in policy discussions due to its extreme nature. SSP3-7.0 is understood as a balanced compromise—sufficiently pessimistic yet in line with current policies. Note that patterns of change are generally consistent across scenarios, differing only in timing and impact intensity. For example, impacts projected under SSP3-7.0 by 2070 (2.8°C warming) are projected to occur by 2060 under SSP5-8.5, given the same level of warming. This approach allows scenarios to be translated by focusing on the warming signal rather than specific timelines. Please see the attached tables, which illustrate the relationship between warming levels and future periods for different scenarios. For more information see: IPCC AR6 https://data.ceda.ac.uk/badc/ar6_wg1/data/spm/spm_08/v20210809/panel_a

CO2 emissions by 2100, a global temperature change of approximately 2.1°C by mid-century (2040–2059) and 2.7°C (likely 2.1°C to 3.5°C) by the end of the century (2080–2099), with respect to pre-industrial conditions (1850–1900).

Historical Temperature Changes

Over the past few decades, mean air surface temperatures have risen significantly, with a notably faster increase observed in the last three decades compared to earlier periods (**Fig. 5**). The temperature trends are as follows: from 1951 to 2020, the trend is 0.11°C per decade; from 1971 to 2020, it increases to 0.16°C per decade; and from 1991 to 2020, the trend further rises to 0.22°C per decade (ERA5 dataset). The largest temperature increase has occurred during the hot season, particularly from December to February, with a trend of 0.18°C per decade from 1971 to 2020, while the other seasons experienced a lower trend of 0.14 to 0.15°C per decade. The minimum and maximum average temperatures are increasing at similar rates overall, although the maximum temperature trend in Anjouan (eastern island) is slightly higher, at 0.19°C per decade over the same period.

FIGURE 5. Historical Average Surface Air Temperature (1950–2023) and Linear Trends for Different Periods as Labelled, ERA5 Dataset



Projected Temperature Changes

Comoros's temperatures are projected to increase further into the future for all the scenarios. Under SSP3-7.0, the mean temperature nationwide increases from 25.31°C during the historical reference period of 1995–2014 to 25.86°C (25.62°C, 10th percentile, 26.25°C, 90th percentile) for the period 2020–2039, and to 26.39°C (26.10°C, 26.98°C) for the period 2040–2059.

Minimum temperature nationwide increases from 24.02°C during the historical reference period to 24.57°C (24.31°C, 24.95°C) for the 2020–2039 period, and 25.09°C (24.79°C, 25.67°C) for 2040–2059. Maximum temperature increases from 26.60°C to 27.15°C (26.91°C, 27.55°C) for the 2020–2039 period, and 27.70°C (27.41°C, 28.27°C) for 2040–2059.

The projected temperature trend from 2000 to 2050 is 0.23°C per decade (for SSP3-7.0), which is a similar rate to that observed historically during the last 3 decades (ERA5 dataset). Warming is projected to continue at an approximately steady rate after 2050 under the SSP3-7.0 scenario. Projected warming under SSP2-4.5 and SSP1-2.6 is lower, and under SSP5-8.5, higher (**Fig. 6**).

FIGURE 6A. Projected Average Mean Surface Air Temperature for Different Climate Change Scenarios as Labeled

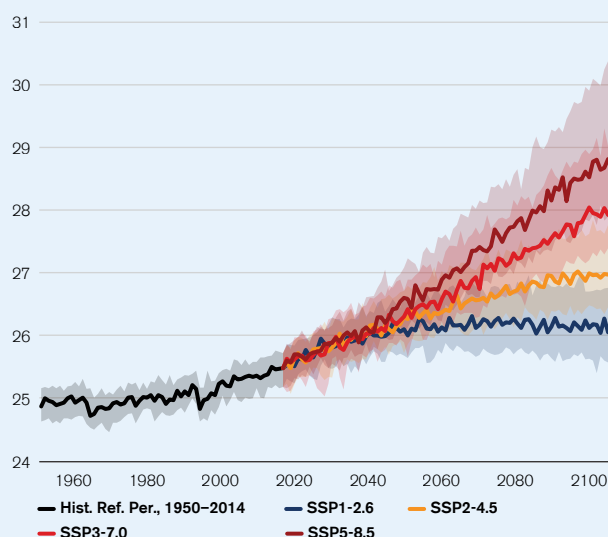
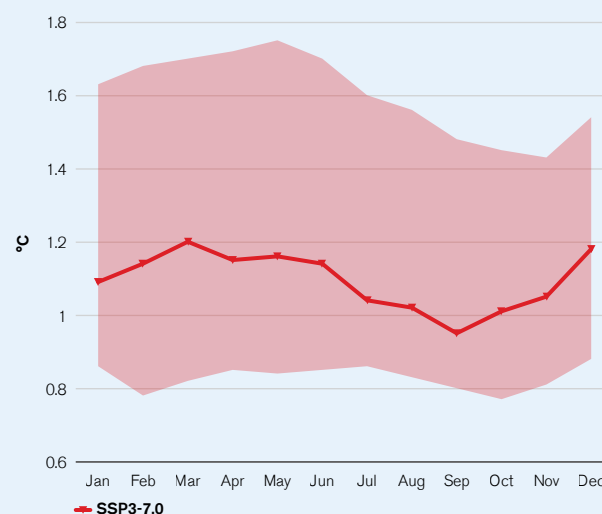


FIGURE 6B. The Projected Monthly Anomaly of the Average Mean Surface Air Temperature for 2040–2059 (relative to the reference period 1995–2014) Under SSP3-7.0, Along with the 10th–90th Percentile Dispersion Across Models



The projected temperature increase is slightly lower in July to November (dry season, transition period from low to higher temperatures) similarly to the historical findings, but note the high uncertainty across models. The minimum and maximum temperatures exhibit similar seasonal trends throughout the year.

Historical Precipitation Changes

The long-term trend indicates a general drying pattern, although the past three decades have shown a slight, though not statistically significant, increase in rainfall (**Fig. 7**). From 1951 to 2020, the trend was a decrease of 25 mm per decade, while the trend from 1971 to 2020 showed a more pronounced decline of 51 mm per decade (4% decrease respect to the ERA5 annual total average over 1990–2020).

Between 1960 and 1975, strong precipitation events were consistently observed in May and June, marking the transition from the rainy to the dry season. However, after this period, there was a significant reduction in rainfall during these months (**Fig. 7**).

Fig. 8 shows the spatial pattern of precipitation change over the 50-year period from 1971 to 2020 in the region. As shown, Comoros has experienced a general decline in precipitation, particularly between March and May—the transition from the wet to the dry season, which indicates a shortening of the rainy season overall.

Note that interannual variability in rainfall is substantial, and the period between 1975 and 2010 experienced a higher frequency of fluctuations compared to the other periods. It is important to note that ERA5 reanalysis data tends to systematically underestimate precipitation compared to station data from CRU, likely due to the difficulty

FIGURE 7A. Historical Precipitation (1950–2022) and Linear Trends for Different Periods as Labelled. ERA5 Dataset.

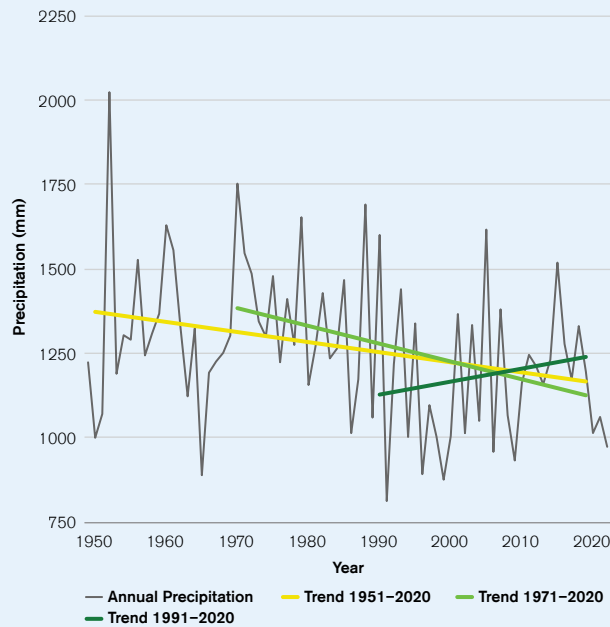


FIGURE 7B. Seasonal Variation in the Intensity of Precipitation Events During the Historical Period. ERA5 Dataset.



on modeling small islands. Nevertheless, ERA5 remains useful for understanding historical trends and variability.

Projected Precipitation Changes

In Comoros, climate change is not projected to significantly affect average annual precipitation levels, and both interannual variability and inter-model dispersion remain notably high (**Fig. 9**). Under SSP3-7.0, Comoros's average annual precipitation is predicted to change minimally nationwide the following decades: from 1235.44 mm (1121.68 mm, 10th percentile, 1376.64 mm, 90th percentile) during the historical period (1995–2014, historical scenario) to 1275.54 mm (1033.86 mm, 1505.34 mm) for 2020–2039, and to 1241.6 mm (1040.11 mm, 1504.1 mm) for 2040–2059.

FIGURE 8. Decadal Precipitation Trend (Total Annual) in the Region, 1971–2020. Significant Trends Include the Decrease Along the Northern Edge of Comoros, As Well as the Increase Towards the Northeast. Comoros Lies on the Southern Edge of the Significant Decrease Patch.

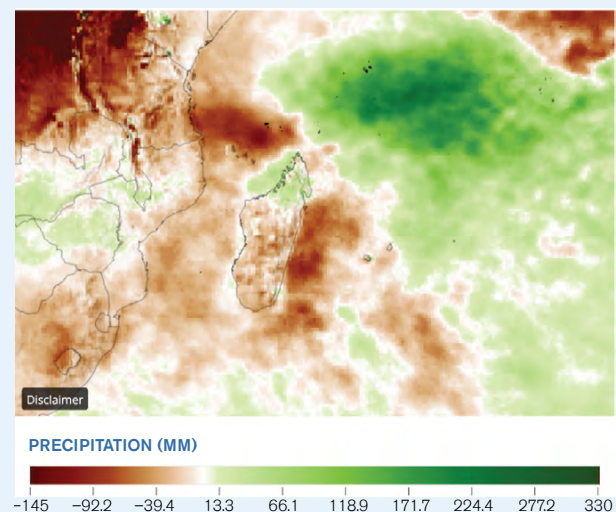


FIGURE 9A. Projected Annual Precipitation for Different Climate Change Scenarios as Labeled

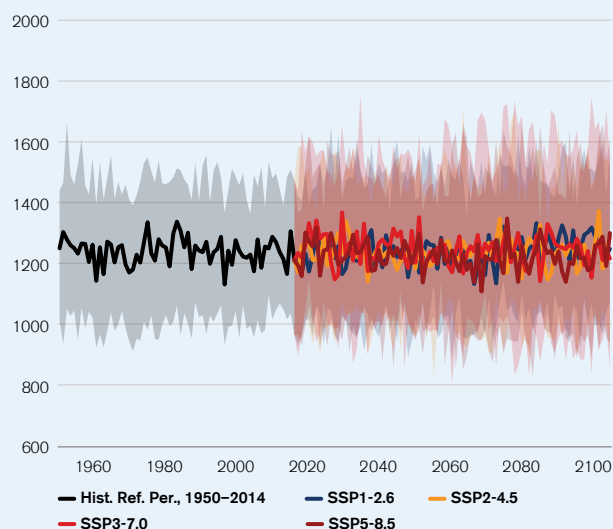
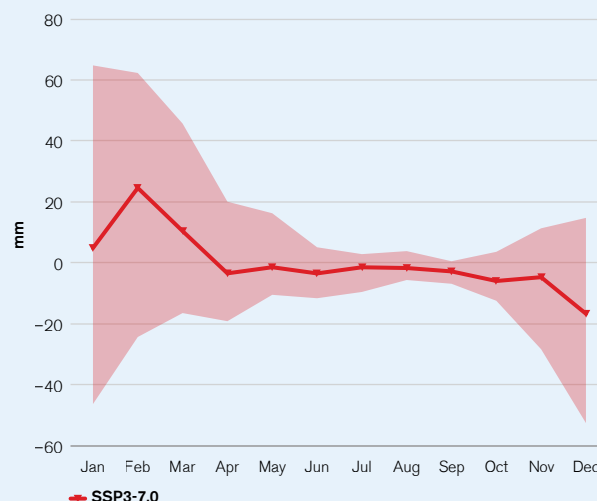
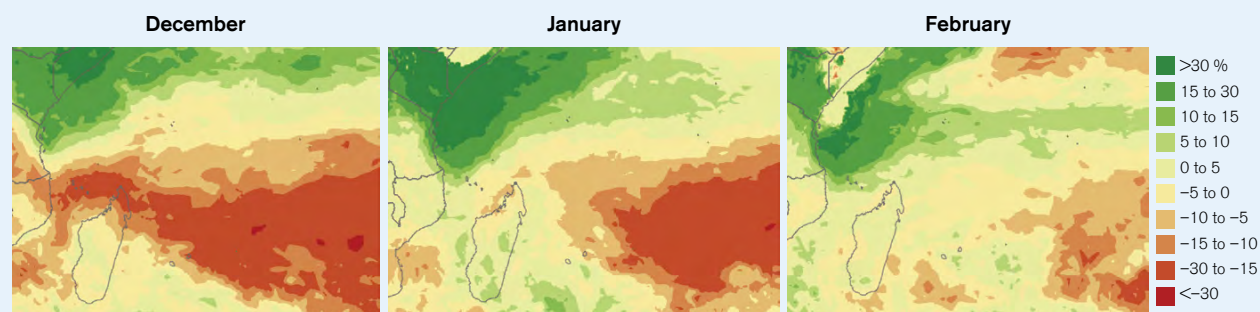


FIGURE 9B. The Projected Monthly Anomaly of Precipitation for 2040–2059 (relative to the reference period 1995–2014) Under SSP3-7.0, Along with the 10th–90th Percentile Dispersion Across Models



However, seasonal changes in precipitation are projected (**Fig. 9b**). During the rainy season, particularly in January and February, precipitation is projected to increase, as shown by the wet pattern moving toward Comoros (**Fig. 10**). In contrast, from September to December, the dry season is expected to become even drier, particularly toward the end in December. This indicates a future climate with a slightly wetter wet season, a drier dry season, and a delayed onset of the rainy season. These shifts could have significant implications for agriculture, water availability, and related sectors.

FIGURE 10. Projected Percent Change in Total Precipitation for (left) December, (center) January (peak precipitation), and (right) February for 2040–2059 with Respect to the Historical Period (1995–2014) for SSP3-7.0



Hot Days

Hot days pose significant risks to both human and animal health, increasing the likelihood of heat-related illnesses, while also heightening the threat of wildfires, damaging crops, straining water supplies, increasing irrigation needs, and driving up energy demand, all of which can disrupt infrastructure, ecosystems, food security, and livelihoods.

By 2040–2050 (SSP3-7.0, CMIP6 models), models predict that every day of the year will be classified as a summer day ($T_{\max} > 25^{\circ}\text{C}$). While nine months in the historical period were already warm (275 days annually) and will continue to warm, climate change will extend summer temperatures into the cooler season from July to September.

The number of hot days ($T_{\max} > 30^{\circ}\text{C}$), insignificant during the historical period, starts increasing rapidly from 2040 due to increasing temperatures, reaching 22.6 days by 2040–2059 and 99.8 days per year by 2080–2099 (more than 3 months). However, temperatures above 35°C are not projected to be reached in Comoros, even by the end of the century.

Hot Nights

Hot nights pose risks to sleep quality, human health, and agricultural crops, as the lack of cooling during the night can exacerbate heat stress on plants, hindering growth and reducing yields, while also increasing the risk of heat-related illnesses, higher energy consumption, and greater strain on power grids.

The number of hot (tropical) nights in Comoros is increasing rapidly. Historically, the island experienced about 38 tropical nights per year ($T_{\min} > 26^{\circ}\text{C}$). Under the SSP3-7.0 scenario, projections show a rise to 75 nights (roughly 2.5 months) annually by 2030 (2020–2039), 120 nights (4 months) by mid-century (2040–2059), and 223 nights (more than 7 months) by the end of the century (2080–2099). Similarly, tropical nights with a lower temperature threshold of 23°C ($T_{\min} > 23^{\circ}\text{C}$) averaged around 265 days annually (almost 9 months) in the historical period. By 2030, this is expected to increase to 298 days (almost 10 months), 322 days (10.5 months) by 2050, and become year-round by 2090. By the century's end, Comoros will experience hot tropical nights ($T_{\min} > 29^{\circ}\text{C}$) 16 days per year.

As illustrated, tropical nights with $T_{\min} > 23^{\circ}\text{C}$ will occur from October to June by 2050 (**Fig. 11a**). By 2090 (**Fig. 11b**), these nights will extend into the typically cooler months of June and October. Moreover, by the century's end, most of the period from December to June will experience even hotter tropical nights, with minimum temperatures surpassing 26°C , and a few of these nights exceeding 29°C .

Next, we examine the percentage of the population at high health risk due to hot nights. High-risk areas are locations where the 50-year return level¹¹ of the annual number of days with night temperatures exceeding 26°C is greater than 30¹². By the mid-term (2010 to 2059, with 2035 as the central year), the entire population in

¹¹ A 50-year return level refers to an event that is expected to occur, on average, once every 50 years.

¹² Population dataset: Gridded Population of the World, Version 4: GPWv4; Revision 11, Dec 2018. For each pixel (at approximately 25 km resolution), the return level for a given return period is calculated by fitting a Generalized Extreme Value (GEV) distribution. A pixel is classified as "too risky" (1) if the return level exceeds the specified threshold, and "not too risky" (0) otherwise. The reported population exposure represents the percentage of the total population in each region that is exposed to risk (1).

FIGURE 11A. Projected Seasonal Cycle of the Number of Tropical Nights, T_{min} Exceeding 23°C, 26°C, 29°C, for SSP3-7.0 by 2040–2059

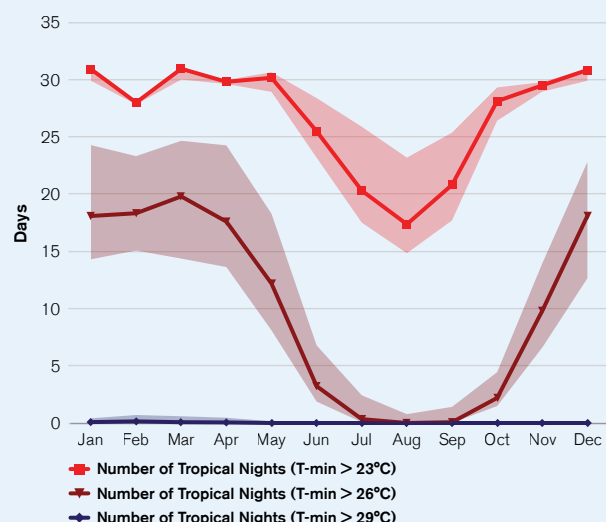
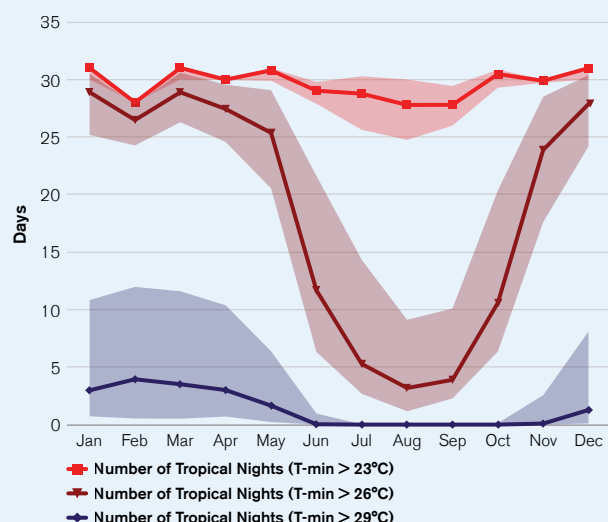


FIGURE 11B. Projected Seasonal Cycle of the Number of Tropical Nights, T_{min} Exceeding 23°C, 26°C, 29°C, for SSP3-7.0 by 2080–2099



Comoros will be exposed to dangerous levels of tropical nights, compared to 37.58% during the historical period (1975–2025). By the end of the century (2050–2099, with 2075 as the central year), 16.31% of the population will face even higher risks, with more than 20 days per year of tropical nights exceeding 29°C at the 50-year return level.

Humid Heat

The Heat Index is a measure of perceived temperature that combines both air temperature and humidity in the shade¹³. When both are high, the Heat Index rises, significantly increasing the risk to human health. In such conditions, the body's ability to cool itself through sweating is impaired, which can lead to heat-related illnesses or even fatalities.

The number of days with a Heat Index of 35°C or higher is expected to become significant around 2050, particularly during the hot months (January to May). For the period 2040–2059, the SSP3-7.0 scenario projects an average of only 5 days per year with a Heat Index above 35°C. From 2051 to 2100, this number is expected to increase by an additional 20.0 days per decade, potentially reaching up to three months per year by 2081–2100 (90.6 days per year).

By 2060–2079 under the SSP3-7.0 scenario, March is projected to experience nearly 10 days with a heat index above 35°C, with a few days exceeding 37°C (left plot in **Fig. 12**). This trend intensifies significantly towards the end of the century (right plot), with approximately two-thirds of February and March expected to see a heat index over 35°C. Around one-third of these months will surpass 37°C, and some days may even exceed heat index 39°C.

¹³ Heat Index as defined by US-National Weather Service - Steadman R.G., 1979: The assessment of sultriness. Part I: A temperature-humidity index based on human physiology and clothing science. J. Appl. Meteorol., 18, 861–873, doi: <http://dx.doi.org/10.1175/1520-0450>

FIGURE 12A. Projected Seasonal Cycle of the Number of Days with a Heat Index Exceeding 35°C, 37°C, 39°C, and 41°C for SSP3-7.0 by 2060–2079

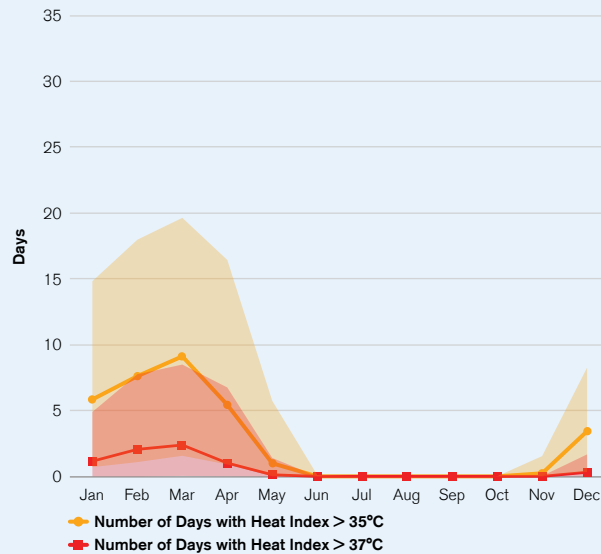
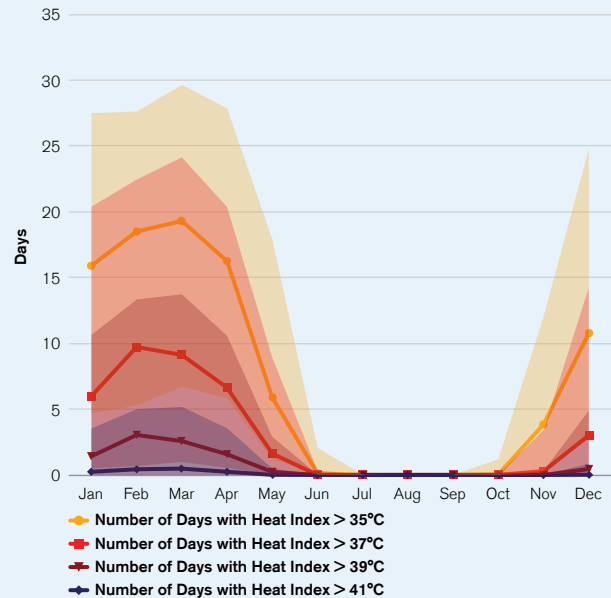


FIGURE 12B. Projected Seasonal Cycle of the Number of Days with a Heat Index Exceeding 35°C, 37°C, 39°C, and 41°C for SSP3-7.0 by 2080–2099



High-risk areas are locations where the 50-year return level of the annual number of days with heat index exceeding 35°C is greater than 20—a threshold considered particularly dangerous for health. For Comoros, this exposure increases from 0% during the period 1975–2025 (historical + SSP3-7.0) to 5% between 2010 and 2059 (central year 2035) to 100% exposure between 2050 and 2099 (central year 2075), so all population are exposed to dangerous heat indices by the end of the century. Moreover, by the end of the century (2050–2099, central year 2075), 100% of the population is projected to be exposed to dangerous wet bulb temperatures under the SSP3-7.0 scenario, where the 50-year return level of the annual number of days with wet bulb temperatures exceeding 27°C is greater than 15. Wet bulb temperatures¹⁴ also indicate extreme heat and humid conditions. The population most at risk will be in Mohéli, the smaller island located in the south.

Drought

Between 1950 and 1965, the yearly maximum number of consecutive dry days¹⁵ ranged from 14 to 28 days (ERA5 dataset, **Fig. 13**). This was followed by a period of shorter droughts, with a maximum duration of 17 days, and in some years, as few as 10 days, until 1990. Since 1990, droughts have varied between 13 and 22 days on average, with the

¹⁴ Wet Bulb Temperature formulation by Stull (2011) - Stull R., 2011: Wet-bulb temperature from relative humidity and air temperature. J. Appl. Meteorol. Climatol., 50(11), 2267–2269, doi: 10.1175/JAMC-D-11-0143-1

¹⁵ This statistic measures the maximum length of a dry spell, computed sequentially for the entire time series, then taking the maximum value during each year in the data period (a dry day is defined as any day in which the daily accumulated precipitation < 1 mm)

exception of a particularly notable 30-day drought in 2015. Although no significant trends are observed for the long-term period from 1950 to 2020 or the more recent period from 1990 to 2020, there is a trend from 1971 to 2020 showing an increase of 1.2 more consecutive dry days per decade. This increase is associated with the period of lower variability and shorter droughts, followed by the occurrence of longer droughts since the 1990s. In summary, the length of droughts has been highly erratic which might be due to modes of climate variability.

Looking ahead, the maximum number of consecutive dry days is projected to increase slightly, from an average of 20.6 days per year during the historical period (1995–2014) to 24.5 days by the end of the century (2080–2099), according to CMIP6 models. However, this projected change is not consistent across all models and is within the interannual variability.

Extreme Precipitation

The yearly maximum number of consecutive wet days¹⁶ has decreased significantly, with a reduction of 2.81 days per decade from 1951 to 2020, and 2.84 days per decade from 1971 to 2020 (**Fig. 14**). This trend reflects an increase in erratic weather patterns and an overall decrease in total precipitation. The maximum number of consecutive wet days dropped from around 50 days per year in 1950 to about 30 days in 2020, despite considerable interannual variability. Between 1980 and 2000, variability declined notably, with the maximum number of consecutive wet days consistently remaining below 40 days, in stark contrast to earlier decades when values reached as high as 90 days. Although variability increased again after 2000, it has not returned to the higher levels observed between 1950 and 1980 (ERA5 data).

¹⁶ This statistic measures the maximum length of a wet spell, computed sequentially for the entire time series, then taking the maximum value during each year in the data period (a wet day is defined as any day in which the daily accumulated precipitation ≥ 1 mm)

FIGURE 13. Yearly Maximum Number of Consecutive Dry Days for the Historical Period (1951–2020) and Linear Trends Over the Labeled Periods, ERA5 Dataset

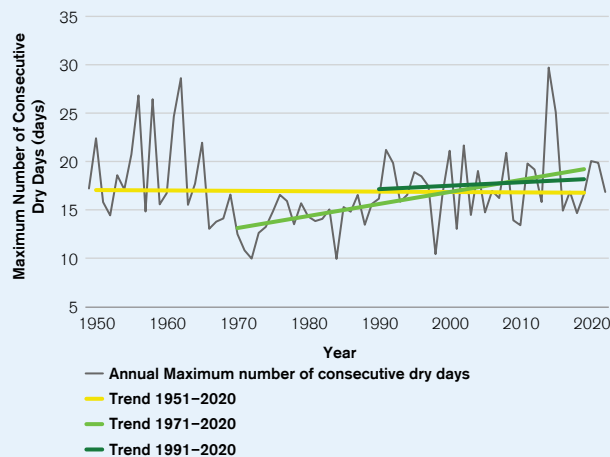
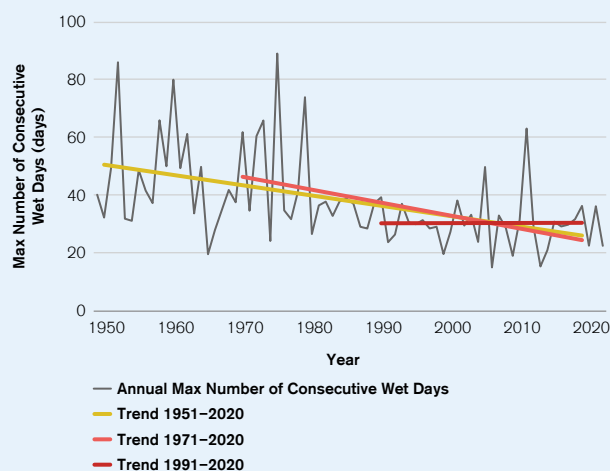


FIGURE 14. Yearly Maximum Number of Consecutive Wet Days for the Historical Period (1951–2020) and Linear Trends Over the Labeled Periods, ERA5 Dataset



However, due to climate change, the maximum number of consecutive wet days is not expected to change significantly in the future, given the interannual and CMIP6 multi-model variability. It is projected to remain around a median of 35 wet days per year, with the 10th and 90th percentiles ranging from 28 to 45 days, as observed during the historical period (1995–2014).

On the other hand, intense and rare precipitation events are expected to become more frequent, with their return periods decreasing. This will likely increase the risk of flooding and pose significant threats to infrastructure, human safety, and agriculture. In Comoros, extreme precipitation events with return periods of 50 and 100 years are projected to occur 50% more often by 2050 (2035–2064) and more than twice as often by the end of the 21st century (2070–2099) under the SSP3-7.0 scenario, compared to historical values from 1985–2014 (**Table 1**). Extreme precipitation events with return periods of 100 years are projected to occur 74% more frequently by mid-century (2035–2064) under the SSP3-7.0 scenario, compared to historical data from 1985–2014. This means that what was historically a 100-year event will occur approximately every 58 years in the future. Similarly, 50-year return events are projected to increase by nearly 58%, 25-year events by 41%, and 10-year events by 30% by mid-century. In Comoros, a 100-year precipitation event corresponds to 163 mm of rain falling in a single day—an amount that, historically, has been observed over an average of 20 days during the rainiest month of January.

TABLE 1. Future (2035–2064) and (2070–2099) Return Period (years) for Extreme Precipitation Events that Correspond to the Return Levels for the Largest Single-Day Event During the Historical Period (1985–2014) for SSP3-7.0. Change in Future Exceedance Probability Expressed as Change Factor for Extreme Precipitation Events that Correspond to the Return Levels for the Largest Single-Day Event During the Historical Period (1985–2014) for Future (2035–2064) and (2070–2099) SSP3-7.0.

Time Period	Historical Return Period (1985–2014, center 2000)					
1985–2014 center 2000	5-yr	10-yr	20-yr	25-yr	50-yr	100-yr
	Future Return Period (years) - Median (10th, 90th percentiles) - SSP3-7.0					
2035–2064 center 2050	4.16 (2.83–5.36)	7.74 (4.96–10.35)	14.21 (8.69–20.88)	17.18 (10.40–26.21)	31.65 (17.92–53.26)	57.72 (29.42–109.59)
2070–2099 center 2085	3.40 (2.20–5.50)	6.17 (3.59–10.73)	11.11 (5.45–20.94)	13.54 (6.09–26.17)	23.79 (8.85–54.03)	41.07 (13.16–120.17)
	Fractional Change - SSP3-7.0 - Median (10th, 90th percentiles) - SSP3-7.0					
2035–2064 center 2050	1.21 (0.92–1.64)	1.30 (0.88–1.85)	1.41 (0.77–2.16)	1.46 (0.73–2.27)	1.58 (0.64–2.70)	1.74 (0.56–3.09)
2070–2099 center 2085	1.48 (0.83–2.20)	1.62 (0.81–2.63)	1.81 (0.79–3.42)	1.86 (0.79–3.70)	2.14 (0.77–4.84)	2.49 (0.71–6.36)

Fractional change above 1 indicates increased probability and decreased return period. For example, a fractional change of 1.74 indicates a 74% increase in the probability of suffering 100-year extreme precipitation events in the future, or 1.74 more likely.

This trend aligns with the Clausius-Clapeyron equation, which states that in a warmer climate, the air's capacity to hold moisture increases exponentially, leading to a higher potential for heavier rainfall. However, the uncertainty in

these projections remains high (see **Table 1**). As a result, the entire population is and will continue to be exposed to dangerous levels of extreme rainfall. High-risk areas are locations where the 50-year return level of the annual largest 5-day precipitation exceeds 130 mm.

Sea Surface Temperatures

Since the 1950s, the Indian Ocean and western boundary currents have experienced the most rapid surface warming. Additionally, there has been a noticeable trend of decreasing salinity in the Indian Ocean¹⁷.

The West Indian Ocean maintains a warm average sea surface temperature of approximately 27°C. Sea surface temperatures typically range from around 26°C in August–September to approximately 28°C in April (historical, 1995–2014, multi-model CMIP6 average). The high temperatures in February and March are known to fuel more intense cyclones. With climate change, the West Indian Ocean is already suffering more marine heatwaves, with fatal consequences for coral reefs and impacts on marine biota. Under the scenario SSP3-7.0, sea surface temperatures are projected to increase 1.2°C (0.9°C, 10th percentile, 1.4°C, 90th percentile) near-term (2021–2040), 1.7°C (1.4°C, 2.1°C) by mid-century (2041–2060), and 3.2°C (2.4°C, 3.9°C) long term (2081–2100), relative to the pre-industrial period (1850–1900)¹⁸.

Sea Level Rise

According to altimetry (satellite) data, sea level rose 12 centimeters total from 1993 to present¹⁹. Under the SSP3-7.0 scenario, sea level is expected to rise 19 centimeters from 2020 to 2050, with a likely range from 13 to 25 centimeters²⁰. This means that by 2050, sea level rise is projected to reach 0.25 meters, and by 2100, it is expected to reach 0.77 meters, under the SSP3-7.0 scenario relative to the historical period (1995–2014) (**Fig. 15**)²¹. Over the next three decades, sea level rise is expected to be roughly the same across all emission and warming scenarios. However, beyond that period, high-emission scenarios predict significantly higher sea level rise. Although there are still high uncertainties, it is certain that sea levels will continue to rise in all scenarios for centuries, driven by the long-term inertia of the oceans. This makes long-term planning essential.

Under the SSP3-7.0 scenario, there is a 92% chance of global sea level rise exceeding half a meter, and a 9% chance of surpassing 1 meter by 2100. This rise in sea levels will contribute to increased inundation. There were 792 days exceeding the minor high-water level between 1980 and 1990, and 1071 between 2005 and 2015 in Comoros. “As sea levels rise, flooding will start to occur more often and with worsening severity”²². The minor high-water level is defined as 40 cm above the average high tide (mean higher high-water, MHHW) and serves as an indicator of potential flooding impacts.

¹⁷ IPCC AR6 WGI, Chapter 9: Ocean, Cryosphere, and Sea Level Change

¹⁸ Data/plots from the IPCC Interactive Atlas WGI, <https://interactive-atlas.ipcc.ch/regional-information>

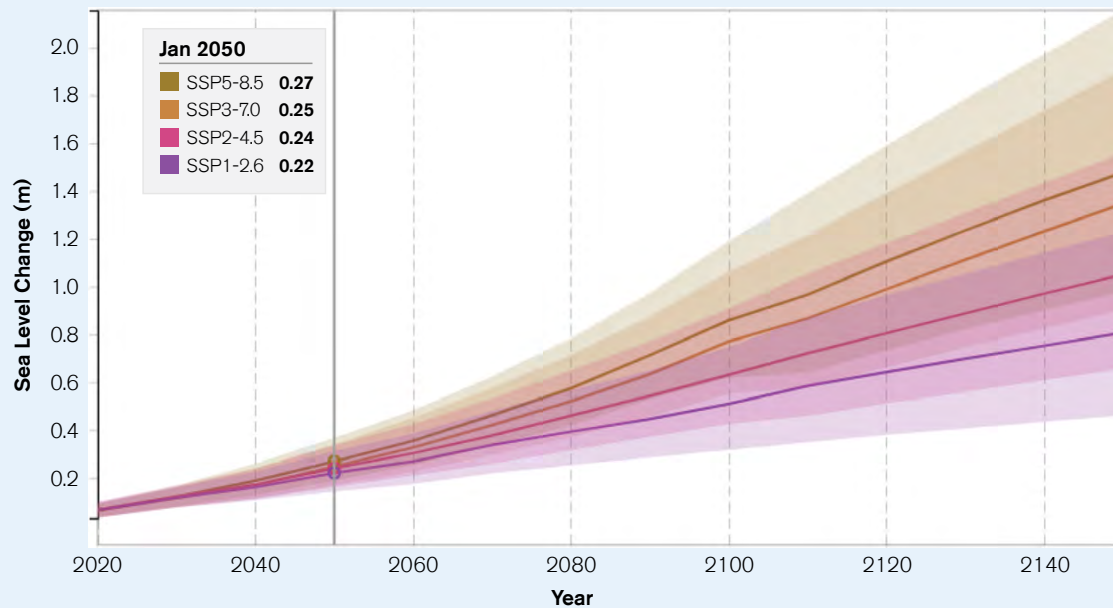
¹⁹ NASA <https://earth.gov/sealevel/sea-level-explorer/>

²⁰ NASA <https://earth.gov/sealevel/sea-level-explorer/>

²¹ NASA https://sealevel.nasa.gov/ipcc-ar6-sea-level-projection-tool?data_layer=scenario&lat=-12&lon=+43 12S, 43E, 1995–2014 baseline

²² NASA <https://earth.gov/sealevel>

FIGURE 15. Projected Total Sea Level Change Under Different SSP Scenarios Relative to the Historical Baseline (1994–2014)²³. The Shaded Ranges Show Uncertainties at 17th–83rd Percentile Ranges.



Note that the human-induced influence on regional sea level changes is expected to become apparent first in areas with relatively low internal variability, such as the tropical Indian Ocean²⁴.

Extreme sea level surge events are projected to become significantly more frequent across much of the tropics. In Comoros, a sea level event with a 100-year return period, currently reaching 2 meters, is expected to occur as often as once every 5–10 years by 2050 under the RCP4.5 scenario, with approximately 2°C of warming²⁵. Tebaldi et al. (2021)²⁶ project that 100-year sea level events will become annual occurrences with just 1.5°C of global warming (in the region near Comoros northwest of Madagascar).

Tropical Cyclones

Comoros lies within the core cyclone band (see **Fig. 16**), which is mostly active from October to May there. Cyclonic events often lead to severe coastal damage, destruction of infrastructure, loss of biodiversity, landslides, and the displacement of communities.

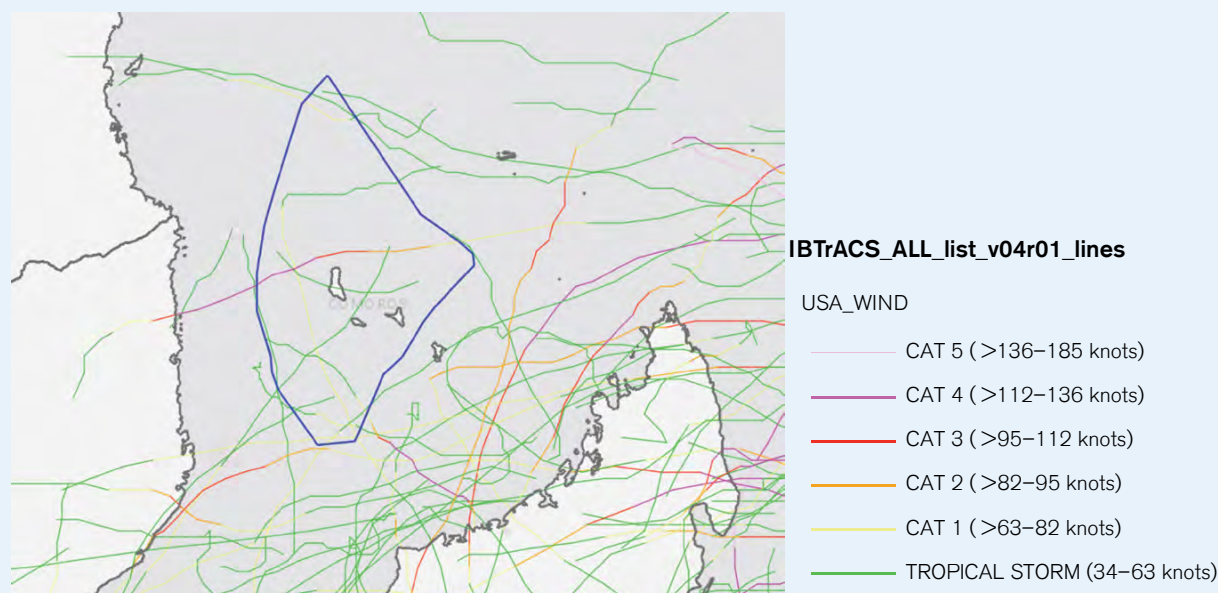
²³ NASA https://sealevel.nasa.gov/ipcc-ar6-sea-level-projection-tool?data_layer=scenario&lat=-12&lon=+43 12S, 43E, 1995–2014 baseline

²⁴ IPCC AR6 WGI, Chapter 9, Ocean, Cryosphere and Sea Level Change

²⁵ Vousdoukas, M.I., Mentaschi, L., Voukouvalas, E. et al. Global probabilistic projections of extreme sea levels show intensification of coastal flood hazard. *Nat Commun* 9, 2360 (2018). <https://doi.org/10.1038/s41467-018-04692-w>

²⁶ Tebaldi, C., Ranasinghe, R., Vousdoukas, M. et al. Extreme sea levels at different global warming levels. *Nat. Clim. Chang.* 11, 746–751 (2021). <https://doi.org/10.1038/s41558-021-01127-1>

FIGURE 16. Observed Historical Cyclones from the International Best Track Archive for Climate Stewardship (IBTrACS)²⁷. All Recorded Cyclones have been Classified According to the Saffir-Simpson²⁸ Scale Using the Variable “USA_wind”, Which Records Sustained Maximum Winds Every 3 Hours (in knots). The IBTrACS Historical Data Covers Cyclones Recorded from 1840 to the Present, with the Caveat that Records Prior to 1980 May Be Incomplete. In Blue, the Exclusive Economic Zone of Comoros.



Data overview: The occurrence of tropical cyclones in any specific location remains a rare event, making historical records too limited to reliably estimate recurrence intervals for these storms. This historical uncertainty can be partially addressed using models that simulate large ensembles of tropical cyclones. One such tool is the Columbia HAZard Model (CHAZ²⁹), which generates an extensive synthetic catalog of potential cyclone tracks by simulating tropical cyclones across the oceans and their impacts upon landfall. This approach provides a more comprehensive perspective compared to observational data alone. The findings presented here rely exclusively on the CHAZ model, utilizing the column relative humidity (CRH) configuration to represent moisture. These simulations are informed by 12 different Global Circulation Models from the CMIP6 ensemble and project tropical cyclone activity during the historical period (1951–2014) and into the future under the SSP2-4.5 scenario, focusing on the period

²⁷ International Best Track Archive for Climate Stewardship (IBTrACS) <https://www.ncei.noaa.gov/products/international-best-track-archive>

²⁸ We classify Tropical Cyclones using the Saffir-Simpson Hurricane Scale, which uses maximum sustained wind speed.

Tropical Storm (green): 34 to <64 knots (63 to <118.5 km/h)

Cat 1 (yellow): 64 to <83 knots (118.5 to <154 km/h)

Cat 2 (orange): 83 to <96 knots (154 to <178 km/h)

Cat 3 (red): 96 to <113 knots (178 to <209 km/h)

Cat 4 (pink): 113 to <137 knots (209 to <254 km/h)

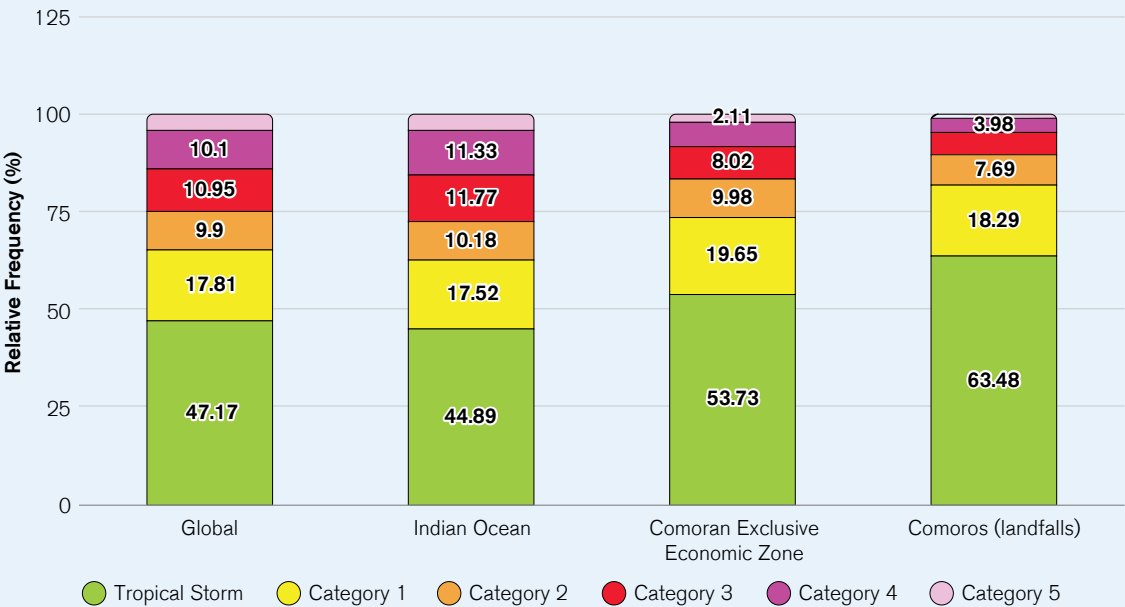
Cat 5 (light pink): ≥137 knots (≥254 km/h)

²⁹ Lee, C.-Y., Tippet, M. R., Sobel, A. H., & Camargo, S. J. (2018). An environmentally forced tropical cyclone hazard model. *Journal of Advances in Modeling Earth Systems*, 10, 223–241. <https://doi.org/10.1002/2017MS001186>

2035–2064 (centered around 2050). We apply a footprint to the CHAZ tracks to capture the full extent of the cyclones. This is especially important for small islands to ensure that the cyclone’s impact is not underestimated. The footprint is based on modeled horizontal wind profiles and latitude, using a dual-exponential decay function derived from 380 observed storms, as detailed by Willoughby et al. (2006)³⁰.

Tropical Cyclones are classified using the Saffir-Simpson Hurricane Scale, which is based on maximum sustained wind speeds (see **Fig. 16**). Historically, the frequency of tropical cyclones (maximum wind speeds above 34 knots) in the entire Comoran Exclusive Economic Zone (EEZ) is 1.6 cyclones per year, corresponding to a return period of 0.62 years. Of these, 0.4 cyclones per year make landfall, equivalent to a return period of about 2.45 years. Slightly above half of the cyclones that intersect with the EEZ are tropical storms (53%), 20% are Category 1 cyclones, and only 2% reach Category 5 intensity. At landfall, the proportion of lower-intensity cyclones increases, with tropical storms accounting for 63%, while the proportion of high-intensity cyclones, such as Category 5, decreases to 1% (**Fig. 17 and Table 2**).

FIGURE 17. Simulated Percentage of Cyclone Types for Global Oceans, Indian Ocean, Comoran Exclusive Economic Zone, Comoros (landfalls), CHAZ, historical (1951–2014)



In this region, the CHAZ model projects a slight, though not significant, increase in high-category cyclones. For Category 5 cyclones, the model predicts a 12% increase in the EEZ (–9% to 31%), with a larger projected increase of 22% at landfall (–7% to 53%). However, there is considerable dispersion across CMIP6 models. What is certain is that sea level surges will increase as a result of the combined effects of ongoing sea level rise and cyclones, even if the frequency or intensity of cyclones does not change.

³⁰ Willoughby, H. E., R. W. R. Darling, and M. E. Rahn, 2006: Parametric Representation of the Primary Hurricane Vortex. Part II: A New Family of Sectionally Continuous Profiles. *Mon. Wea. Rev.*, 134, 1102–1120, <https://doi.org/10.1175/MWR3106.1>.

TABLE 2. Median Value (with 10th and 90th percentiles) of Counts of Cyclones per Year for Historical (1951–2014) and Projected Future Period (2035–2064, central year 2050) Along with the Fractional Changes for the Full EEZ Area and for Landfall (<1 means a decrease in the frequency of storms, >1 means an increase in the frequency of storms). Note That the Reported Median of Fractional Change is Not Necessarily the Future Median Divided by the Historical Median Value. Values are Rounded to One Thousandths.

	Comoran Exclusive Economic Zone			Comoros (landfalls)		
	Historical Cyclone Count per Year	SSP2-4.5 Cyclone Count per Year	SSP2-4.5 Fractional Change	Historical Cyclone Count per Year	SSP2-4.5 Cyclone Count per Year	SSP2-4.5 Fractional Change
Category 5	0.034 (0.017, 0.040)	0.035 (0.023, 0.041)	1.120 (0.910, 1.310)	0.004 (0.003, 0.006)	0.005 (0.004, 0.007)	1.220 (0.930, 1.530)
Category 4	0.105 (0.055, 0.116)	0.105 (0.075, 0.120)	1.110 (0.810, 1.260)	0.016 (0.010, 0.019)	0.018 (0.014, 0.023)	1.120 (0.780, 1.400)
Category 3	0.130 (0.082, 0.142)	0.126 (0.105, 0.141)	0.990 (0.750, 1.270)	0.023 (0.014, 0.025)	0.024 (0.018, 0.028)	1.090 (0.840, 1.360)
Category 2	0.161 (0.105, 0.174)	0.153 (0.126, 0.171)	0.940 (0.710, 1.220)	0.031 (0.021, 0.035)	0.032 (0.022, 0.038)	1.020 (0.730, 1.390)
Category 1	0.317 (0.232, 0.341)	0.295 (0.258, 0.349)	0.930 (0.750, 1.300)	0.075 (0.058, 0.081)	0.076 (0.055, 0.085)	0.970 (0.690, 1.330)
Tropical Storm	0.868 (0.708, 0.951)	0.834 (0.736, 0.942)	0.940 (0.870, 1.190)	0.259 (0.235, 0.283)	0.254 (0.202, 0.277)	1.000 (0.800, 1.160)
Total	1.615 (1.199, 1.765)	1.548 (1.323, 1.764)	0.970 (0.810, 1.240)	0.408 (0.341, 0.449)	0.409 (0.314, 0.458)	1.030 (0.770, 1.230)

The IPCC AR6 report³¹ states that in a warming world, the average and maximum rainfall rates associated with tropical cyclones (TCs), extratropical cyclones, atmospheric rivers, and severe convective storms in some regions are projected to increase (high confidence). Peak rainfall rates from TCs are expected to rise with local warming, at least at the rate of mean water vapor increase over oceans (approximately 7% per 1°C of warming), and in some cases, may exceed this rate due to increased low-level moisture convergence driven by stronger TC winds (medium confidence). It is likely that the global proportion of Category 3–5 tropical cyclones has increased over the past four decades. As global warming intensifies, the proportion of intense TCs, average peak TC wind speeds, and the peak wind speeds of the most intense TCs will continue to rise (high confidence). However, the total global frequency of TC formation is expected to either decrease or remain unchanged with increasing global warming (medium confidence).

Caveat: The predictability of future tropical cyclones is accompanied by significant uncertainties due to several factors. These include discrepancies between climate models, the inherent complexity of processes integrated into Tropical Cyclone Models, and regional variations in cyclone formation, behavior, and dispersal. Furthermore, Tropical Cyclone Models are predominantly calibrated for current climate conditions, which could introduce additional

³¹ IPCC WGI Chapter 11: Weather and Climate Extreme Events in a Changing Climate

biases when applied to future scenarios. In summary, the complex and often conflicting interactions among ocean temperatures, wind patterns, and atmospheric conditions that drive cyclone formation, movement, and landfall are still not fully understood, making it difficult to predict which trends will ultimately dominate. For further details on the current understanding of tropical cyclones and their frequency, refer to Sobel et al. (2021)³².

Blue Economy Impacts

The main critical marine ecosystems in Comoros are coral reefs, seagrass beds and mangrove forests. These provide multiple benefits to biodiversity, fisheries, blue carbon, and resilience to floods.

The IPCC AR6 WGII Chapter 15 on Small Islands³³ states that coral reefs are most at risk. “Scientific evidence has confirmed that globally and in small islands tropical corals are presently at high risk (high confidence). Severe coral bleaching, together with declines in coral abundance, has been observed in many small islands, especially those in the Pacific and Indian oceans (high confidence).”

By the period 2090–2099 and under the high-emissions scenario RCP8.5 (+4.4°C), marine animal biomass along Comoros’ coast is expected to decline up to 8% (Tittensor et al., 2021³⁴), relative to levels observed during 1990–1999.

The historical maximum sustainable yield from 2012 to 2021 is 14 metric tons for Comoros entire Exclusive Economic Zone. By 2100, under the RCP8.5 scenario (with a projected warming of +4.5°C), the maximum sustainable yield is expected to decrease slightly by 3% compared to historical levels (Free et al., 2020³⁵).

Temperate tuna species such as albacore, Atlantic bluefin, and southern bluefin are anticipated to decline in tropical regions (where Comoros is part of) and migrate poleward. Conversely, skipjack and yellowfin tunas are expected to increase in abundance within tropical areas (Erauskin-Extramiana et al., 2019)³⁶.

Trisos et al. (2020)³⁷ project that as climate change advances, the risks to biodiversity will intensify, potentially leading to a catastrophic loss of global biodiversity. Using temperature and precipitation projections from 1850 to 2100, they assess the exposure of over 30,000 marine and terrestrial species to hazardous climate conditions. The study predicts that climate change will abruptly disrupt ecological assemblages, as most species within any

³² Sobel, A. H., Wing, A. A., Camargo, S. J., Patricola, C. M., Vecchi, G. A., Lee, C.-Y., & Tippett, M. R. (2021). Tropical cyclone frequency. *Earth's Future*, 9, e2021EF002275. <https://doi.org/10.1029/2021EF002275>

³³ Chapter 15 - Small Islands, IPCCWG2, https://www.ipcc.ch/report/ar6/wg2/downloads/report/IPCC_AR6_WGII_Chapter15.pdf

³⁴ Tittensor, D.P., Novaglio, C., Harrison, C.S. et al. Next-generation ensemble projections reveal higher climate risks for marine ecosystems. *Nat. Clim. Chang.* 11, 973–981 (2021). <https://doi.org/10.1038/s41558-021-01173-9>

³⁵ Free CM, Mangin T, Molinos JG, Ojea E, Burden M, Costello C, et al. (2020) Realistic fisheries management reforms could mitigate the impacts of climate change in most countries. *PLoS ONE* 15(3): e0224347. <https://doi.org/10.1371/journal.pone.0224347>

³⁶ Erauskin-Extramiana M, Arrizabalaga H, Hobday AJ, et al. Large-scale distribution of tuna species in a warming ocean. *Glob Change Biol.* 2019; 25: 2043–2060. <https://doi.org/10.1111/gcb.14630>

³⁷ Trisos, C.H., Merow, C. & Pigot, A.L. The projected timing of abrupt ecological disruption from climate change. *Nature* 580, 496–501 (2020). <https://doi.org/10.1038/s41586-020-2189-9>

given assemblage will simultaneously face conditions beyond their niche limits. Under a high-emissions scenario (RCP 8.5), these abrupt exposure events are expected to begin before 2030, with tropical oceans, including the Comoros, being particularly affected.

Tropical small islands have particularly rich ecosystems. Protecting biodiversity is essential for adapting to climate change, among other reasons (e.g. Sala et al., 2021³⁸ or Zhao et al., 2020³⁹).

³⁸ Sala, E., Mayorga, J., Bradley, D. et al. Protecting the global ocean for biodiversity, food and climate. *Nature* 592, 397–402 (2021). <https://doi.org/10.1038/s41586-021-03371-g>

³⁹ Zhao et al. (2020), Where Marine Protected Areas would best represent 30% of ocean biodiversity, *Biological Conservation*, Volume 244, 108536, <https://doi.org/10.1016/j.biocon.2020.108536>

CLIMATE RISK COUNTRY PROFILE

COMOROS



THE WORLD BANK
IBRD • IDA | WORLD BANK GROUP